Adaptive color rendering for images containing flesh tone content

Minghui Xia[1] Eli Saber[2] A. Murat Tekalp[1]
Gaurav Sharma[2]

[1]Electrical Engineering Department and Center for Electronic Imaging Systems
University of Rochester, Rochester, NY 14627

[2]Xerox Corporation, 800 Phillips Road, Webster, NY 14580

ABSTRACT

A novel color rendering algorithm for printing images with flesh tone content is addressed in this paper. Instead of rendering the whole image with one Color Rendering Dictionary (CRD), two CRDs, a global CRD and a flesh tone CRD are employed to correct the image adaptively. First, the optimal CRD for flesh-tone is designed by densely sampling, in color space, the flesh tone region and selecting special Neugebauer primaries. Then, a given image is segmented into flesh-tone and non-flesh-tone regions. The flesh-tone region is corrected by utilizing the flesh-tone CRD while the remainder of the image is corrected by employing the global CRD. The resulting separation of cyan, magenta, yellow and black could be sent directly to printer or could be compressed and stored for later use. The quality of the flesh tone content in an image will be improved by using optimally designed CRD for flesh tone while the rest of the image is corrected by the global CRD.

Keywords: adaptive color rendering, color printer calibration, color rendering dictionary

1. INTRODUCTION

In order to produce color images on a hardcopy, device calibration is needed to compensate for the characteristics of the printer. Currently, a Color Rendering Dictionary (CRD) is utilized to convert an image from a device independent color space into a device dependent one. The procedure for calibrating a printer can be summarized as follows. First, a set of color patches are printed and measured. To this effect, the measurement data are employed to characterize the printer, thereby generating generate a multi-dimensional mapping from device control values (e.g. CMYK) to colors specified in a device-independent color space (e.g. CIEXYZ or CIELAB). Then the resulting characterization function is inverted to form a CRD which encompasses, in the form of a look-up-table (LUT), an appropriate strategy for color space conversion, under-color removal (UCR) / gray component replacement (GCR)*, and generation of tone reproduction curves (TRC). The CRD, thereafter, is applied globally to the entire image as a form of color correction.

It is always desirable to design a CRD as accurate and dense as possible for generating high quality images. However, this is infeasible, in practice, due to the computational complexity and formidable storage requirements. As an alternative solution, it is possible to enhance the quality of special regions in an image by utilizing separate CRDs to render the color of those regions. For instance, the flesh tones in an image would be printed at a higher quality if the flesh tones were processed by utilizing a separate CRD designed to optimize the reproduction of flesh tones while other regions are processed by utilizing a global CRD. The advantage of utilizing two separate CRDs over making only one CRD more dense is that the region of special interest may occupy very small volume in the color space (e.g. CIELAB space). It is clear that global dense sampling will cause too much unnecessary cost in storage .

The special topic of generating a separate CRD for processing flesh tones is addressed in this paper because people usually pay close attention to flesh tones in a pictorial image.[1,2] However, it should be noted that using a specially

Email- M.X: xia@ee.rochester.edu; E.S: Eli_Saber@xn.xerox.com; A.M.T: tekalp@ee.rochester.edu; G.S: sharma@wrc.xerox.com

*Under-color Removal (UCR) or Gray Component Replacement (GCR) is a technique where the gray component of a three col or image is replaced during reproduction with a corresponding level of black. The advantage of using the black printer is to produce better blacks and be more efficient in using the toner.

designed CRD need not be restricted to flesh tones rendering. Any region of special interest to the viewer could be processed by optimally designed CRD for that region. The proposed method for rendering color images can be accomplished in three steps. First, an optimal CRD for flesh tone rendering (flesh-tone CRD) is designed. Then the image to be rendered is segmented into flesh-tone regions and non-flesh-tone regions. The optimally designed flesh-tone CRD is then applied to the flesh-tone regions while the global CRD is applied to other regions to obtain correct device dependent color control values. The block diagram of the whole algorithm is illustrated in Fig. 1. Details of these steps are described in the following sections.

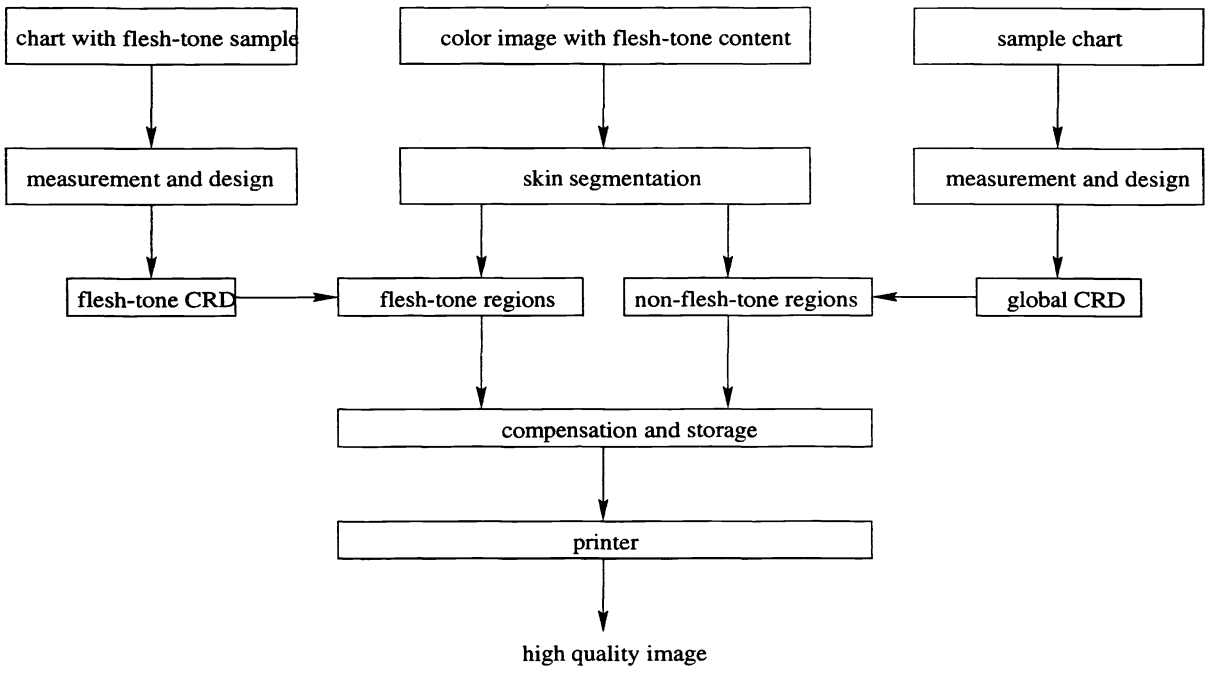

Figure 1. Block diagram of color rendition for images with flesh tone content

2. IMAGE SEGMENTATION

In order to render an image adaptively, it is first necessary to segment the image into different regions. specifically, skin region and non-skin region. The segmentation is performed in the CIELAB color space. CIELAB color space is selected because: 1), the major difference between human skin and other objects is their chroma, which can be represented by $a^\star - b^\star$ values in the CIELAB space, and 2), of its international status as a standard accepted in most color systems. It should be noted that the change in illumination conditions may change the brightness of an object represented by $L^\star$. Therefore, the segmentation need only be performed in $a^\star - b^\star$ plane. Indeed, the $a^\star - b^\star$ plane can be divided into two regions: skin region and non-skin region. In the CIELAB color space, a pixel is said to belong to skin class if its projection onto the $a^\star - b^\star$ plane falls into the skin region, otherwise it belongs to the non-skin class. The segmentation algorithm is based on the assumption that the distribution of pixels in $a^\star - b^\star$ plane belonging to skin class can be viewed as a random process, which could be modeled by a two dimensional Gaussian function, characterized by its mean vector and covariance matrix. That is, the chrominance vector at a pixel (m,n), which belongs to skin class, can be represented by the mean chrominance vector of skin class plus a zero-mean Gaussian residual.[3,4] Specifically, suppose we have two hypothesis:

$$\begin{aligned} H_0 &: \text{The pixel belongs to skin class} \\ H_1 &: \text{The pixel doesn't belong to skin class} \end{aligned} \tag{1}$$

Let $\mathbf{i}_{mn}$ denote the vector composed of the a^* and b^* components for the pixel at site (m,n). Furthermore, let $\boldsymbol{\mu}_s$ and $\mathbf{Q}_s$ denote the color mean vector and covariance matrix respectively for skin class. Then the probability that a pixel falls into the skin region is computed as follows:

$$p(\mathbf{i}_{mn} \mid H_0(m,n)) = \frac{1}{(2\pi)^{n/2}|\mathbf{Q}_s|^{1/2}} exp(-\frac{1}{2}[\mathbf{i}_{mn} - \boldsymbol{\mu}_s]^T \mathbf{Q}_s^{-1}[\mathbf{i}_{mn} - \boldsymbol{\mu}_s]) \tag{2}$$

where:

$$\mathbf{i}_{mn} = [a^*{}_{mn} \;\; b^*{}_{mn}]^T, \boldsymbol{\mu}_s = [\mu_s^{a^*} \;\; \mu_s^{b^*}]^T, \;\; \mathbf{Q}_s = \begin{bmatrix} (\sigma_s^{a^*})^2 & (\sigma_s^{a^*b^*})^2 \\ (\sigma_s^{a^*b^*})^2 & (\sigma_s^{b^*})^2 \end{bmatrix}$$

and

$$p(\mathbf{i}_{mn} \mid H_1(m,n)) = 1 - p(\mathbf{i}_{mn} \mid H_0(m,n)) \tag{3}$$

Therefore, we can determine whether a pixel belongs to the skin class by performing a Likelihood Ratio Test (LRT). That is, by computing $p(\mathbf{i}_{mn} \mid H_0(m,n))$, we will know the probability of that pixel belonging to skin class. The mean vector $\boldsymbol{\mu}_s$ and the covariance matrix $\mathbf{Q}_s$ for the function can be estimated from appropriate training sets which are selected from subregions in several images containing only pixels belonging to skin class.

The contours of the PDFs in Eq. (2) defines ellipses

$$[\mathbf{i}_{mn} - \boldsymbol{\mu}_s]^T \mathbf{Q}_s^{-1}[\mathbf{i}_{mn} - \boldsymbol{\mu}_s] = \rho_{mn} \tag{4}$$

in the a^*-b^* domain, whose centers and principal axes are determined by $\boldsymbol{\mu}_s$ and $\mathbf{Q}_s{}^{-1}$. The distribution of pixels from the training sets in a^*-b^* space is shown in Fig. 2.

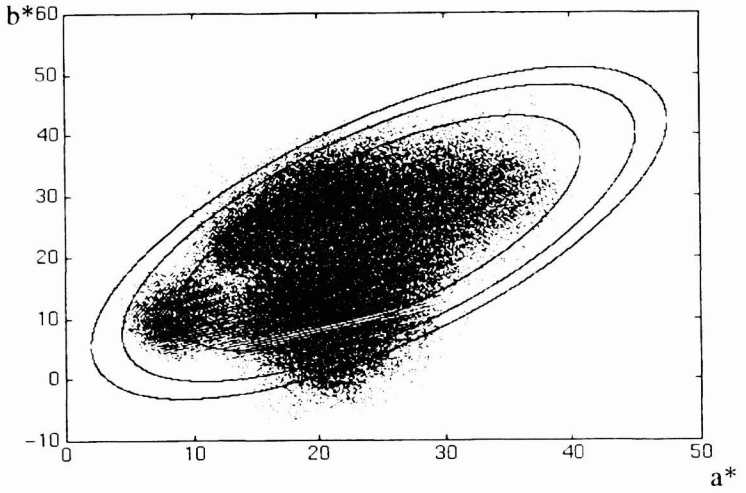

Figure 2. Distribution of skin pixels in $a^* \sim b^*$ space

Using Eq. (4), we can calculate ρ_{mn} at each pixel site (m,n), given $\boldsymbol{\mu}_s$ and $\mathbf{Q}_s$, that are estimated from appropriate training sets. The value of ρ_{mn} is proportional to the probability that pixel (m,n) belongs to the skin class, as can be seen from Eq. (4). A small value of ρ_{mn} indicates that the color of pixel (m,n) is "near" the center of the ellipse, and thereby very likely to belong to the skin class. On the contrary, a large value of ρ_{mn} signifies that it is "far" from the center of the ellipse and its probability of belonging to skin class is small.

Thus, the criterion of segmentation can be easily determined by the following LRT test:

$$\rho_{mn} \underset{H_1}{\overset{H_0}{\lessgtr}} \tau \tag{5}$$

where H_0 and H_1 are defined in Eq. (1) . The threshold τ can be computed using images in the training sets, which provides us with an interval $[0,\tau]$. A pixel with ρ_{mn} within this interval is likely to be a member of skin class.

In addition to employing the LRT in Eq. (5) to perform the classification as described previously, it was observed that most pixels belonging to skin class are bounded by certain chrominance angles denoted by $\tan^{-1}(\frac{a^*}{b^*})$. Therefore, by establishing an upper and lower bound on the chrominance angle, the outcome of the classification can be enhanced. Again, the bound can be obtained from appropriate training set. Thereby, those pixels passing the LRT shown in Eq. (5) and whose chrominance angles fall within the empirically established upper and lower bounds are assigned to the skin class. All others are classified as non-skin pixels. As a result, the final classification can be viewed as an intersection between the end result of the LRT and the outcome of the chrominance angle classification.

3. OPTIMAL DESIGN OF GLOBAL CRD AND FLESH TONE CRD

The first step of designing a CRD is to find a characterization function of the printer, which provide mapping from device dependent color space to device independent color space. Then inverse mapping is performed to construct the CRD, which will be utilized to convert an image from a device independent color space into a device dependent one.

3.1. Utilization of Neugebauer model in global CRD design

In designing a global CRD, Neugebauer model is employed to characterize the printer. Given the parameters of the model, it can be utilized to predict any 'output' of a printer (in the form of device independent color values) from the device control values (in the device dependent color space). For a four-colorant digital halftone printer with cyan (C), magenta (M), yellow (Y) and black (K), the tristimulus of any printed color can be predicted by the tristimuli of $2^4 = 16$ possible combinations of the four colorants, which are called Neugebauer primaries. Since the model was first introduced by Neugebauer in 1937,[5] the model has been extended by several other researchers.[6–8] Specifically, the spectral Neugebauer model (in contrast to the broad band model) and the Yule-Nielsen correction greatly improve the accuracy of the model. Indeed, the spectral reflectance of a printed color patch can be computed from weighted combination of the 16 primaries:

$$R(\lambda) = [\sum_{i=1}^{16} w_i R_i{}^{1/n}(\lambda)]^n, \tag{6}$$

where $R(\lambda)$ denotes the spectral reflectance of the printed patch, λ denotes the spectral wavelength, $R_i(\lambda)$ denotes the reflectance of the Neugebauer primaries, which belong to the set $\mathbf{P}$:

$$R_i(\lambda) \in \mathbf{P} = \left\{ \begin{array}{l} R_W(\lambda), R_C(\lambda), R_M(\lambda), R_Y(\lambda), R_K(\lambda), R_{CM}(\lambda), R_{CY}(\lambda), R_{CK}(\lambda), R_{MY}(\lambda), \\ R_{MK}(\lambda), R_{YK}(\lambda), R_{CMY}(\lambda), R_{CMK}(\lambda), R_{CYK}(\lambda), R_{MYK}(\lambda), R_{CMYK}(\lambda) \end{array} \right\}$$

and R_W stands for the reflectance of paper white. w_i denotes the fractional areas of the primary R_i, which can be computed from a probabilistic model first suggested by Demichel,[9] and is given by:

$$w_i \in \left\{ \begin{array}{l} (1-c)(1-m)(1-y)(1-k), c(1-m)(1-y)(1-k), m(1-c)(1-y)(1-k), \\ y(1-c)(1-m)(1-k), k(1-c)(1-m)(1-y), cm(1-y)(1-k), \\ cy(1-m)(1-k), ck(1-m)(1-y), my(1-c)(1-k), mk(1-c)(1-y), \\ yk(1-c)(1-m), cmy(1-k), cmk(1-y), cyk(1-m), myk(1-c), cmyk \end{array} \right\}$$

where c, m, y, k are relative dot areas of the four colorants that produce the desired color. Normally, the relationship between c, m, y, k and digital values C, M, Y, and K used to drive the printer is quite nonlinear, which need to be determined by measuring sweeps of colorants (in digital value). n represents the empirically determined Yule-Nielsen factor which accounts for the penetration and scattering of light in paper, known as the *Yule-Nielsen effect.*[6]

After predicting the reflectance of the printed patch, CIELAB values can be computed by CIE specified equations.[10] Thus, a characterization function of the printer can be established, which provides mapping from the device dependent color space to the device independent color space. An inverse mapping is then employed to construct the global CRD.

3.2. Optimal skin CRD design by employing cellular Neugebauer model

An extension of the Neugebauer model would be addition of "partial dot area" primaries to the various combinations of only 0% and 100% colorant primaries. In particular, if 0%, 50% and 100% colorant and their combinations are used, up to $3^4 = 81$ primaries will be employed in the Neugebauer model, and the use of 0%, 25%, 50% and 100% colorants will produce $5^4 = 625$ primaries. This is equivalent to partitioning the CMYK space into a set of rectangular cells and applying the Neugebauer model within each cell. Therefore, this model is called the cellular Neugebauer model.[11]

Suppose an arbitrary color patch with digital values C, M, Y, K and resulting relative dot areas c, m, y, k, which represents a point in CMYK color space, falls in a rectangular cell. Let c_l and c_u denote the lower and upper extrema of the cell (in the sense of dot area) along the cyan axis that satisfy:

$$0 \leq c_l \leq c \leq c_m \leq 1, \tag{7}$$

Then, in order to use the cellular Neugebauer model, normalization of c is carried out by:

$$c' = \frac{c - c_l}{c_u - c_l}, \tag{8}$$

and the same procedure generates m', y' and k'. The Neugebauer model is thus applied to this cell by:

$$R(\lambda) = [\sum_{i=1}^{16} w_i'(R_i')^{1/n}(\lambda)]^n, \tag{9}$$

where

$$R_i(\lambda) \in \left\{ \begin{array}{l} R_{c_l m_l y_l k_l}(\lambda), R_{c_u m_l y_l k_l}(\lambda), R_{c_l m_u y_l k_l}(\lambda), R_{c_l m_l y_u k_l}(\lambda), R_{c_l m_l y_l k_u}(\lambda), \\ R_{c_u m_u y_l k_l}(\lambda), R_{c_u m_l y_u k_l}(\lambda), R_{c_u m_l y_l k_u}(\lambda), R_{c_l m_u y_u k_l}(\lambda), R_{c_l m_u y_l k_u}(\lambda), \\ R_{c_l m_l y_u k_u}(\lambda), R_{c_u m_u y_u k_l}(\lambda), R_{c_u m_u y_l k_u}(\lambda), R_{c_u m_l y_u k_u}(\lambda), R_{c_l m_u y_u k_u}(\lambda), R_{c_u m_u y_u k_u}(\lambda) \end{array} \right\}.$$

In designing the flesh tone CRD, the cellular Neugebauer model is employed to characterize the printer. However, the primaries are selected adaptively to accommodate the flesh tone region in the CMYK color space. That is, the color space is divided into non-uniform cells rather than uniform cells. The concept of selecting primaries adaptively to design the flesh-tone CRD is illustrated in Fig. 3. For convenience, only two dimensional color space (C-M) is drawn. C_L and C_U denote the lower and upper boundary of flesh tone on cyan axis. Similarly, M_L and M_U denote the lower and upper boundary of flesh tone on magenta axis. Two sets of primaries are selected. One set is at the four corners of the whole printer gamut. Another set is at the four corners of the flesh tone region. It is easy to extend the idea to the four dimensional color space. After characterizing the printer, the flesh tone CRD can be constructed within the flesh tone region, which may be more densely sampled compared with the global CRD. It should be noted that the two CRDs are designed with an overlapping region within the color space, where their respective nodes are matched (as depicted in Fig. 3). This is necessary to avoid introducing color correction artifacts within the image due to discontinuities along the borders spanned by the skin and global CRDs.

The optimal design method for flesh-tone CRD is described as follows. First, a set of color patches are printed and measured. Some flesh tone samples are provided to optimize the design. Then, the color patch measurements are employed to generate the flesh tone CRD by utilizing Neugebauer cellular model. Note that the color primaries

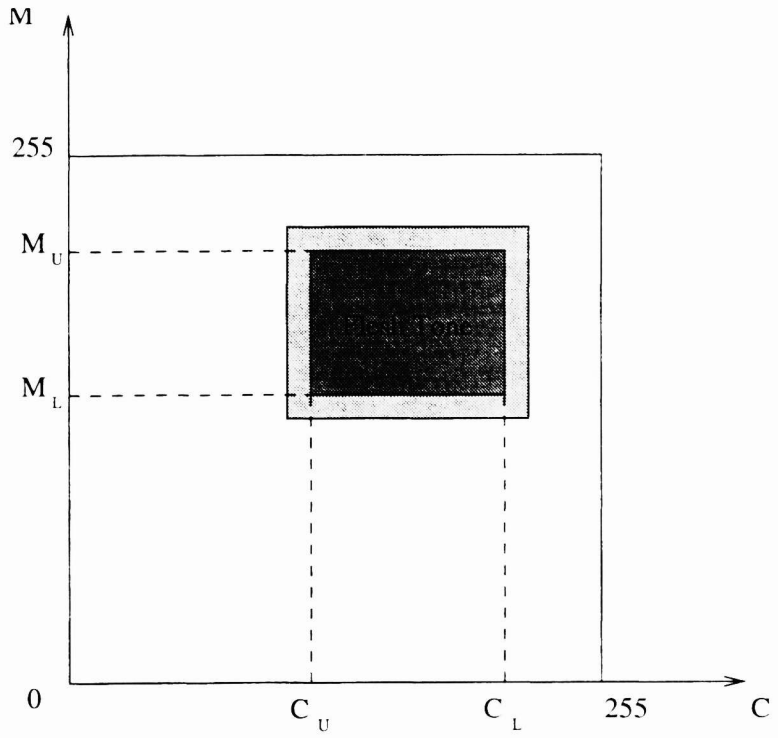

Figure 3. Rendering a portrait image with two CRDs

are specially selected (to contain only flesh-tone region in color space) in this approach to optimize the flesh-tone CRD. Once an image is segmented into two regions, the flesh-tone regions could be processed by optimally designed flesh-tone CRD while the non-flesh-tone regions are processed by the global CRD. The resulting cyan, magenta, yellow and black separations could be sent directly to printer or compressed and stored for later use.

4. RESULTS

The segmentation algorithms were first trained with several portrait images and then tested on some other different images. Two test images are shown in Fig. 4 and Fig. 5 (the color images are shown in gray levels). The segmentation results shown in Fig. 4 were obtained by implementing LRT in Eq. (5). The results shown in Fig. 5 were obtained by implementing LRT and putting additional chrominance angle constraints during the segmentation. It can be observed that the constraints have helped to reduce the number of false assignment of pixels belonging to other regions (e.g. the men's clothes in the lower image) to skin class. However, there are still some mis-assignment in the results, which may be reduced by considering spatial relationship between pixels.

The global CRD and a flesh-tone CRD were designed as described in Section 3. The portrait image is rendered as follows. The global CRD is applied to the whole image for the first rendition. For the second rendition, the image is segmented into skin regions and non-skin regions. Then the global CRD and the flesh-tone CRD are applied to the two types of regions respectively. Significant improvement has been observed on the printing quality of flesh-tone by the second rendition.

5. CONCLUSIONS

An adaptive color rendering scheme for images containing flesh tone content is proposed. A flesh tone CRD and a global CRD are optimally designed. An image is first segmented into flesh-tone regions and non-flesh-tone regions. Then the flesh tone CRD and the global CRD are applied to these regions separately. The rendering quality of the flesh tone content has been improved by this scheme.

REFERENCES

1. F. H. Imai, N. Tsumura, H. Hanneishi, and Y. Miyake, "Prediction of color reproduction for skin color under different illuminants based on color appearance models," *Journal of Imaging Science and Technology* **41**(2), pp. 166–173, 1997.
2. Y. Miyake, H. Saitoh, H. Yaguchi, and N. Tsukada, "Facial pattern detection and color correction from television picture for newspaper printing," *Journal of Imaging Technology* **16**(5), pp. 165–169, 1990.
3. E. Saber, A. M. Tekalp, R. Eschbach, and K. Knox, "Automatic image annotation using color classification," *Graphical Models and Image Processing* **8**, pp. 3–20, March 1996.
4. T. N. Pappas, "An adaptive clustering algorithm for image segmentation," *IEEE Trans. Signal Proc.* **SP-40**, pp. 901–914, April 1992.
5. H. E. J. Neugebauer, "Die theoretischen Grundlagen des Mehrfarbenbuchdrucks," *Zeitschrift für wissenschaftliche Photographie Photophysik und Photochemie* **36**, pp. 73–89, Apr. 1937. reprinted in.[12]
6. J. A. C. Yule and W. J. Nielsen, "The penetration of light into paper and its effect on halftone reproduction," in *TAGA Proc.*, pp. 65–76, 7-9 May 1951.
7. J. A. S. Viggiano, "The comparison of radiance ratio spectra: Assessing a model's "goodness of fit"," in *Adv. Printing of Conf. Summaries: SPSE's 43rd Annual Conference, Rochester, NY*, pp. 222–225, 20-25 May 1990.
8. R. Balasubramanian, "Accuracy of various types of neugebauer models," in *Proc. IS&T and SID's Color Imaging Conference: Transforms and Transportability of Color*, pp. 32–37, Nov. 1993.
9. E. Demichel in *Procédé*, vol. 26, pp. 17–21,26–27, 1924.
10. CIE, "Colorimetry." CIE Publication No. 15.2, Central Bureau of the CIE, Vienna, 1986.
11. K. J. Heuberger, Z. M. Jing, and S. Persiev, "Color transformations and lookup tables," in *1992 TAGA/ISCC Proceedings*, vol. 2, pp. 863–881, 1992.
12. K. Sayangi, ed., *Proc. SPIE: Neugebauer Memorial Seminar on Color Reproduction*, vol. 1184, SPIE, Bellingham, WA, 14-15 Dec. 1989.

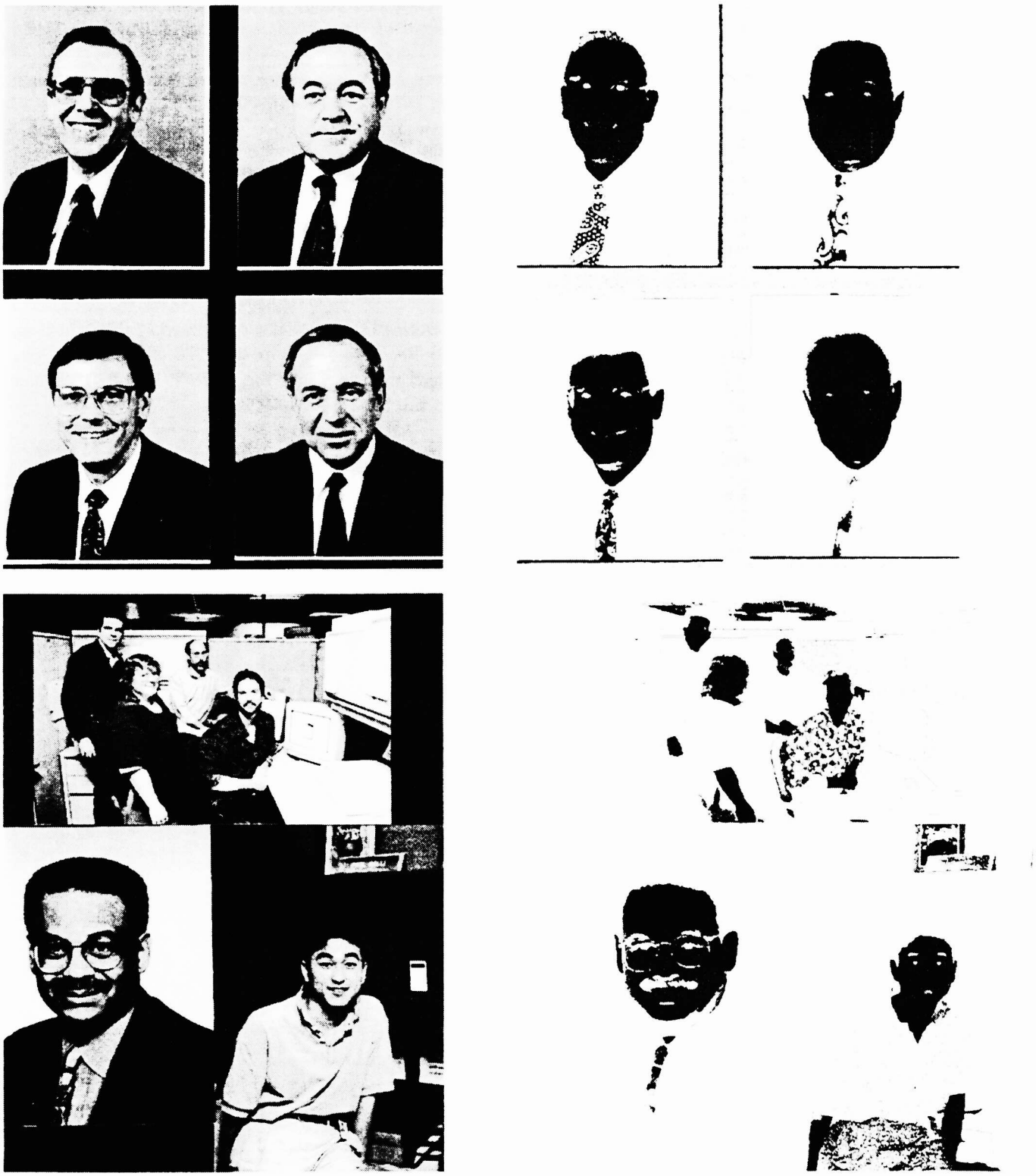

Figure 4. Segmentation without chrominance angle constraint (left: original images; right: after segmentation)

Figure 5. Segmentation with chrominance angle constraint (left: original images; right: after segmentation)